DOI: 10.1002/cbic.200500168

Synthesis and Biological Evaluation of Novel Eg5 Inhibitors

Vasiliki Sarli,[a] Stefan Huemmer,[b] Nils Sunder-Plassmann,[a] Thomas U. Mayer,*[b] and Athanassios Giannis*[a]

*Human Eg5 is a mitotic kinesin that is essential for bipolar spindle formation and maintenance during mitosis. Recently, the discovery of compounds that inhibit Eg5 and cause mitotic arrest has attracted great interest, due to their potential use as the next generation of antimitotics. Here, we present the synthesis and biological investigation of 3,4-dihydrophenylquinazoline-2(1*H*)-thiones as selective and potent Eg5 inhibitors.*

Introduction

During mitosis, eukaryotic cells are organised into a very complex and dynamic structure, the mitotic spindle, which facilitates and ensures the equal partitioning of the replicated chromosomes. Inhibition of mitotic-spindle formation has been identified as an interesting target in cancer chemotherapy.[1] Antimitotic agents that have been used so far in cancer treatment, such as for taxanes and vinca alkaloids, perturb tubulin polymerisation/depolymerisation, cause mitotic arrest and subsequent cell death.[2] However, these drugs produce serious side effects, because microtubules also have essential intracellular functions in nondividing cells.[3] A new, alternative approach to attacking mitotic-spindle formation is the inhibition of proteins, such as the mitotic motors (kinesins), that interact with microtubules; this causes mitotic arrest.[4] These proteins are exclusively involved in the formation and function of the mitotic spindle, and some of them are only expressed in proliferating cells.[5] Their inhibition leads to cell-cycle arrest and ultimately to apoptosis, without interfering with other microtubule-dependent processes.[1] Human Eg5 kinesin or HsKSP, for example, is a plus-end-directed mitotic motor that belongs to the BimC kinesin super-family and is required for the formation of bipolar spindles in vivo.[6] Failure of Eg5 function leads to cell-cycle arrest in mitosis.

The first identified Eg5 inhibitor was monastrol (**1**), a small cell-permeable compound that induces mitotic arrest, thus giving a characteristic monoaster phenotype.[7] Other Eg5 inhibitors that have been reported are dihydropyrazoles (IC_{50} = 26 nM),[8] terpendole E (IC_{50} = 14.6 μM),[9] *S*-trityl-L-cysteine (IC_{50} = 1.0 μM),[10] HR22C16 (IC_{50} = 0.8 μM)[11] and CK0106023 (IC_{50} = 12 nM).[12] Recently, we reported dimethylenastron (**2**; IC_{50} = 200 nM) as a potent and cell-permeable Eg5 inhibitor.[13] We have shown that cyclisation of the side chains of monastrol leads to conformationally restricted bicyclic systems that have strong inhibitory activity against Eg5. In continuation of these studies and supported by data from the molecular-modelling program MOLOC,[14,15] we envisaged the synthesis and biological investigation of 3,4-dihydrophenylquinazoline-2(1*H*)-thiones of type **3**.

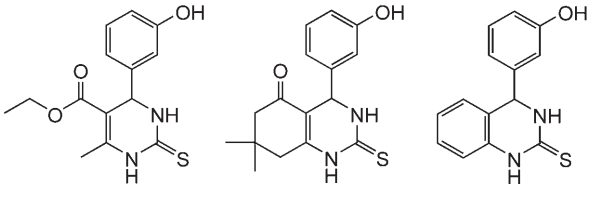

1 2 3

Results and Discussion

The general synthetic strategy shown in Scheme 1 was employed for the preparation of the new 3,4-dihydrophenylquinazoline-2(1*H*)-thiones. A conceptually attractive approach to these thioureas is through commercially available or synthesised aminobenzophenones **7**. As a first step, we synthesised isatoic anhydrides **5** from anthranilic acids **4** by treatment with trichloromethyl chloroformate.[16] Reaction of isatoic anhydrides with *N*,*O*-dimethylhydroxylamine gave Weinreb amide precursors **6** in good to excellent yields. Then we synthesised 2-aminobenzophenones **7** by one-pot reaction of *N*-methoxy-*N*-methylamides **6** and an arylbromide in the presence of *n*BuLi.[17] Such a route proved to be efficient and gave access to 2-aminobenzophenone derivatives with a different substitution pattern in both aromatic rings. Further reduction of the carbonyl group in the presence of $NaBH_4$ generated the intermediate alcohols, which, without isolation upon treatment

[a] *V. Sarli,[+] N. Sunder-Plassmann, Prof. A. Giannis*
University of Leipzig, Institute for Organic Chemistry
Johannisallee 29, 04103, Leipzig (Germany)
Fax: (+49) 341-973-6599
E-mail: giannis@chemie.uni-leipzig.de

[b] *S. Huemmer,[+] T. U. Mayer*
Max Planck Institute for Biochemistry
Chemical Genetics, Independent Research Group
Am Klopferspitz 18, 82152 Martinsried/Munich (Germany)
Fax: (+49) 89-8578-3138
E-mail: mayer@biochem.mpg.de

[+] *These authors contributed equally to this work.*

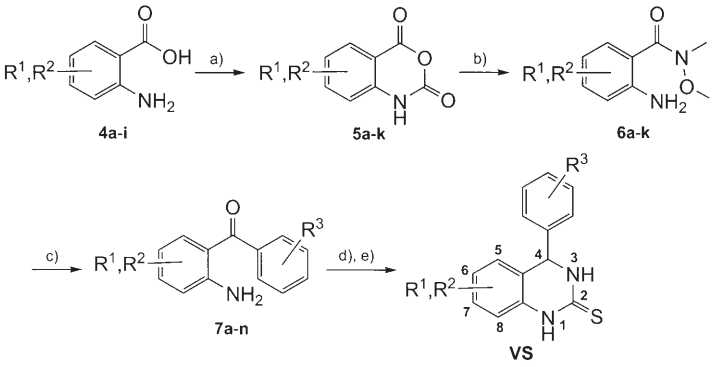

Scheme 1. Reagents and conditions: a) $ClCOOCCl_3$, 1,4-dioxane, reflux, 6 h; b) MeNHOMe. HCl, Et_3N, EtOH, reflux, 2 h; c) *m*-$TBDMSOC_6H_4Br$ (TBDM = *tert*-butyldimethylsilyl), *n*BuLi, THF; −80 °C, 30 min; d) $NaBH_4$, EtOH, 65 °C, 1.5 h; e) NH_4SCN, H_2O, EtOH, HCl, 65 °C, 2 h.

with ammonium thiocyanate and hydrochloric acid, afforded the racemic thioureas **VS** (Table 1).[18]

Subsequently, the synthesised compounds were screened for inhibition of Eg5 by using an in vitro malachite green ATPase assay.[19] Nine of these compounds were more potent inhibitors than monastrol, and their inhibitory effects were quantified by measuring their IC_{50} values (Figure 1). Compounds VS-1, VS-43 and VS-46, gave inhibition values of 6, 38 and 24%, respectively, at a concentration of 50 μM. From these data, it appears that a hydroxyl group on the 3′-position of the 3,4-dihydro-4-phenylquinazoline-2(1*H*)-thione skeleton is important for inhibition. This observation is in accordance with our previous results from a similar system for the development of dimethylenastron.[13] Methyl substitution at position 7 increases the inhibitory activity and is more favourable than halogen substitution. On the other hand, a methyl group at position 9 dramatically decreases the activity. Fluorine groups at positions 6 and 8 gave the most potent compounds, while the 7,8-difluoro derivative is slightly less active. Additionally, we assessed the effect of these compounds on other human motor

Table 1. Precise structures of VS compounds and the intermediates in their formation.

Compounds	R^1	R^2	R^3
4a–7a	5-Cl	H	3′-OTBDMS
4b–7b	3-OMe	H	3′-OTBDMS
4c–7c	4-F	H	3′-OTBDMS
4d–7d	5-F	H	3′-OTBDMS
4e–7e	6-F	H	3′-OTBDMS
4f–7f	4-F	5-F	3′-OTBDMS
4g–7g	3-Me	H	3′-OTBDMS
4h–7h	4-Me	H	3′-OTBDMS
4i–7i	5-Me	H	3′-OTBDMS
5j[a], **6j**, **7j**	5-Br	H	3′-OTBDMS
5k[a], **6k**, **7k**	H	H	3′-OTBDMS
7l[a]	5-Cl	H	H
7m[a]	5-Cl	H	2′-F
7n[a]	H	H	H
VS-42	6-Cl	H	3′-OH
VS-48	8-OMe	H	3′-OH
VS-54	7-F	H	3′-OH
VS-77	6-F	H	3′-OH
VS-83	5-F	H	3′-OH
VS-87	6-F	7-F	3′-OH
VS-38	8-Me	H	3′-OH
VS-91	7-Me	H	3′-OH
VS-94	6-Me	H	3′-OH
VS-17	6-Br	H	3′-OH
VS-12	H	H	3′-OH
VS-43	6-Cl	H	H
VS-46	6-Cl	H	2′-F
VS-1	H	H	H

[a] Commercially available.

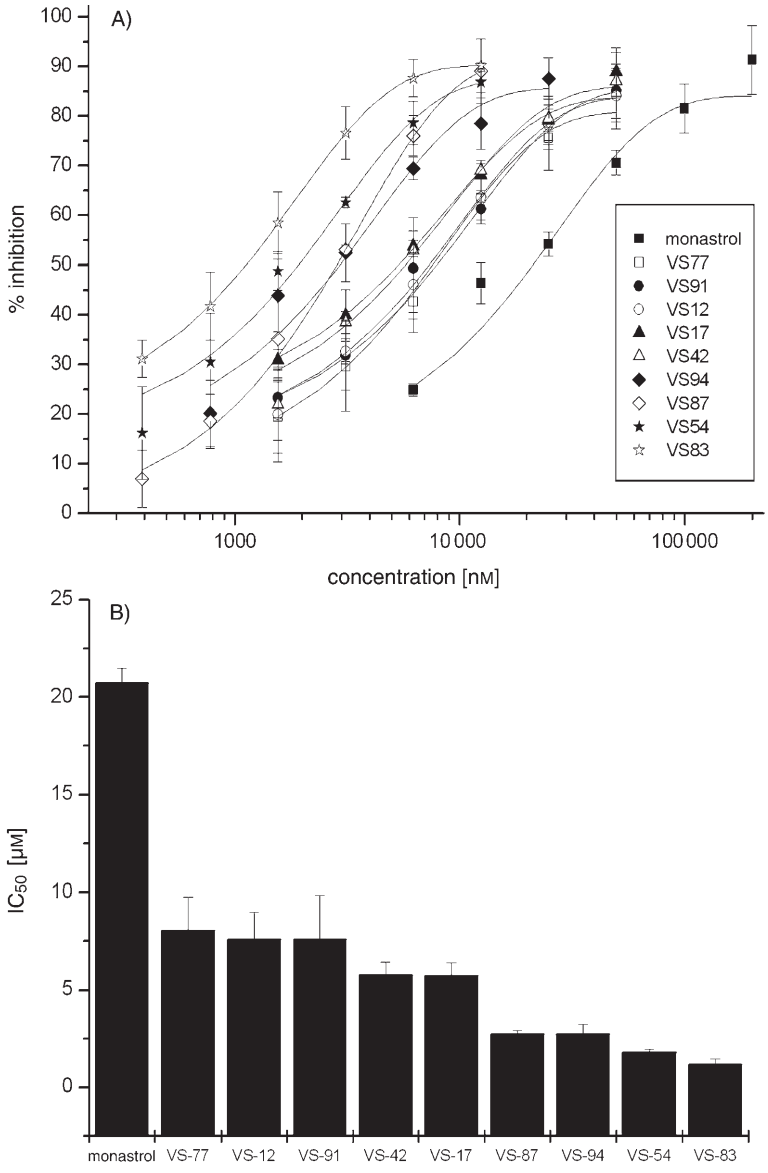

Figure 1. A) VS compounds inhibit the in vitro ATPase activity of mitotic kinesin Eg5 more potently than monastrol does. A malachite green reaction was used to measure the microtubule-stimulated ATPase activity of Eg5 in the presence of the indicated concentration of VS compounds or monastrol. The in vitro ATPase activity of Eg5 in the presence of the solvent control, DMSO, was set to 100% activity. B) Graph A was used to determine the concentration of each compound at which the in vitro ATPase activity of Eg5 was half maximal (IC_{50} value).

proteins including MKLP1, MKLP2, MPP1, KIF4, KIF5A, KIF5B, CenpE and MCAK. We found that the induced inhibition was specific for Eg5 (data not shown).

Flow cytometric analysis was used to examine the cell-cycle distribution of compound-treated BSC-1 cells that were stained with Hoechst dye to visualise the chromatin.[20] BSC-1 cells synchronised in the S-phase were released into 10 μM of each inhibitor with 500 nM of nocodazole or DMSO as a solvent control, and the cell-cycle profiles of the treated cells were determined by using a laser-scanning microscope. Analyses of the cell-cycle profile revealed that 500 nM nocodazole blocked cells efficiently in G2/M phase. In line with the determined IC_{50} values, compounds VS-94, VS-87, VS-54 and VS-83 induced a block at G2/M phase more efficiently than equimolar concentrations of VS-12, VS-17, VS-42, VS-77 or monastrol (Figure 2, Table 2).

To further confirm that the determined in vitro potencies of the compounds correlate with their efficiency to induce a phenotype in vivo, we quantified the number of compound-treated mitotic cells displaying monoasters or bipolar spindles. BSC-1 cells synchronised in the S-phase were released for 10 h into the indicated concentrations of VS compounds or monastrol, and the number of mitotic cells displaying monoasters was determined. Based on the graph shown in Figure 3 A, we determined for each compound the concentration at which 50% of the mitotic cells showed monoasters (EC_{50}). As shown in Figure 3 B, the EC_{50} values of the individual compounds exactly correlate with the potencies of the compounds inhibiting Eg5 ATPase activity in vitro; this demonstrates that the VS compounds are membrane-permeable inhibitors of Eg5 that cause a mitotic arrest in vivo by inducing monoasters in treated cells.

Finally, we observed spindle morphologies in BSC-1 cells arrested with 25 μM VS-83 and 100 μM monastrol (Figure 4). VS-83 arrested cells in mitosis with monoastral microtubule arrays, a phenotype identical to that induced by monastrol or microinjection of inhibitory-acting antibodies against Eg5.

Conclusion

Mitotic kinesin inhibitors offer a novel approach to inhibiting proliferation of cancer cells[12,21] with fewer side-effects on non-dividing cells compared to known antitubulin drugs.[22] In this work, we have developed an easy and efficient access to different 3,4-dihydro-4-(3′-hydroxyphenyl)quinazoline-2(1*H*)-thiones, which proved to be potent and specific molecules for Eg5 inhibition. These new antimitotics are promising drug candidates for the treatment of cancer and other proliferative diseases. For these Eg5 inhibitors we propose the name Vasastrol (VS).

Experimental Section

Chemistry. All materials were obtained from commercial suppliers and used without further purification. Melting points were uncorrected and were determined on a Büchi Melting Point B-540 apparatus. Flash chromatography was performed on Merck silica gel 60. ^1H and ^{13}C NMR spectra were recorded on Varian VXR-200, Varian VXR-300 NMR spectrometers at room temperature. High-resolution (HR) mass spectra were obtained with a 7 T APEX II mass spectrometer. Yields are not optimised.

General procedure for the synthesis of isatoic anhydrides 5 a–k: The anthranilic acid (1 equiv), trichloromethyl chloroformate (4 equiv) and anhydrous 1,4-dioxane (3 mL mmol^{-1}) were mixed in a three-necked, round-bottomed flask and heated at reflux under Ar for 6 h. The reaction mixture was allowed to cool to RT, and the flask was connected to a series of tree traps. The first and last traps contained sulfuric acid and 10% potassium hydroxide, respectively, and the middle trap was left empty. Then Ar was bubbled through the reaction mixture for 1 h. The solvent was removed under reduced pressure, and the crude isatoic anhydrides were used for the next step without further purification.

CAUTION! Trichloromethyl chloroformate is toxic.

General procedure for the synthesis of *N*-methoxy-*N*-methylamides 6 a–k: Triethylamine (1.5 equiv) was added to a solution of *N*,*O*-dimethylhydroxylamine hydrochloride (1.5 equiv) in 90% aqueous ethanol (1.75 mL mmol^{-1}), and, after 10 min, isatoic anhydride (1 equiv) was added in portions. The reaction mixture was heated at reflux for 2 h, then poured into an equal volume of saturated $Na(CO_3)_2$. The ethanol was then removed, and the aqueous mixture was extracted with ethyl acetate. The organic extracts were washed with water and brine and dried over Na_2SO_4. The solution was concentrated, and the residue was chromatographed on silica gel.

General procedure for the synthesis of aminobenzophenones 7 a–n: *n*BuLi (2.5 M, in hexane, 2 equiv) was added with vigorous stirring to a mixture of arylbromide (1 equiv) and *N*-methoxy-*N*-methylamide (1 equiv) in dry tetrahydrofuran (6 mL mmol^{-1}) at −80 °C under Ar. The temperature of the reaction mixture should not be higher than −78 °C. After 30 min, aqueous HCl (1 N, 2 mL mmol^{-1}) was added, and the mixture was extracted with ethyl acetate. The organic extracts were washed with water and brine, dried over Na_2SO_4 and concentrated. The residue was chromatographed on silica gel.

General procedure for the synthesis of quinazoline-2(1*H*)-thiones VS: $NaBH_4$ (0.5 equiv) was added portionwise at 65 °C under Ar to a solution of aminobenzophenone (1 equiv) in ethanol (2.3 mL mmol^{-1}). The mixture was heated at 65 °C for 1.5 h, then it was diluted with water (0.36 mL mmol^{-1}), and a solution of ammonium thiocyanate (1.1 equiv) in water (0.16 mL mmol^{-1}) was added at 65 °C. The reaction mixture was then treated with concentrated HCl in water (0.14 mL mmol^{-1}, 0.26 mL mmol^{-1}) and stirred at 65 °C for 2 h. Solvents were removed under reduced pressure, and the residue was chromatographed after preabsorption on silica gel.

2-Amino-5-chloro-*N*-methoxy-*N*-methylbenzamide (6 a): Yield: 89% for two steps. M.p. = 69–72 °C; ^1H NMR (200 MHz, $CDCl_3$): δ = 3.33 (s, 3 H), 3.57 (s, 3 H), 4.56 (br, 2 H), 6.63 (d, J = 8.6 Hz, 1 H), 7.12 (dd, J = 2.5, 8.6 Hz, 1 H), 7.35 (d, J = 2.5 Hz, 1 H); ^{13}C NMR (50 MHz, $CDCl_3$): δ = 35.9, 63.3, 119.9, 120.2, 123.4, 130.7, 133.3, 147.4, 170.6; ESI-HRMS *m/z* calcd for $C_9H_{12}ClN_2O_2$: 215.05818 $[M+H]^+$; found: 215.05835.

2-Amino-*N*,3-dimethoxy-*N*-methylbenzamide (6 b): Yield: 88% for two steps. Oil. ^1H NMR (300 MHz, $CDCl_3$): δ = 3.30 (s, 3 H), 3.57 (s, 3 H), 3.82 (s, 3 H), 4.77 (br, 2 H), 6.61 (t, J = 7.9 Hz, 1 H), 6.77 (d, J = 7.7 Hz, 1 H), 6.96 (d, J = 7.9 Hz, 1 H); ^{13}C NMR, 75 MHz ($CDCl_3$): δ = 34.5, 55.7, 61.1, 111.4, 115.9, 117.0, 120.9, 137.4, 147.5, 170.0; ESI-HRMS *m/z* calcd for $C_{10}H_{15}N_2O_3$: 211.10772 $[M+H]^+$; found: 211.10776.

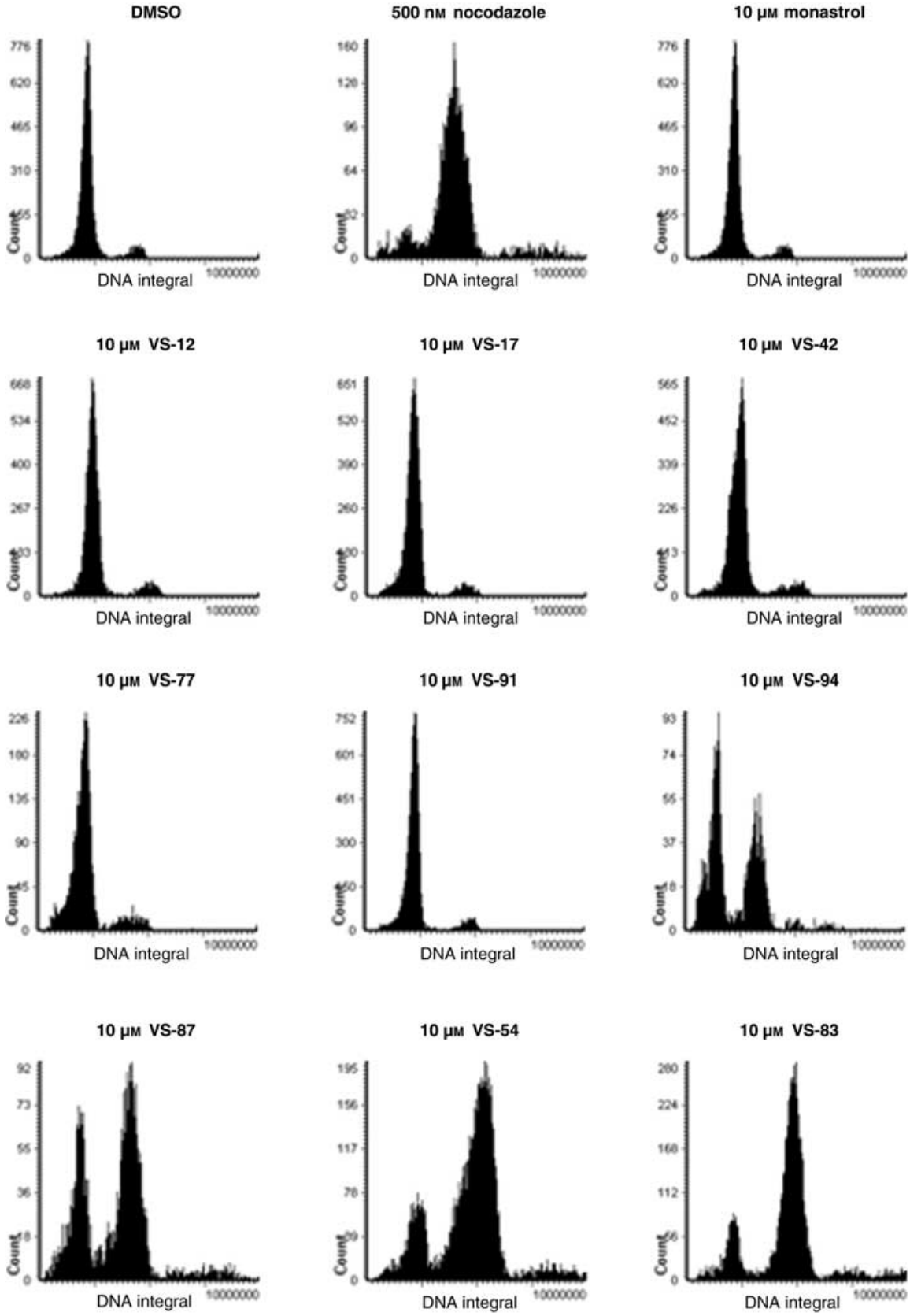

Figure 2. VS-compounds induce mitotic arrest in BSC-1 (African green monkey) cells more potently than monastrol does. BSC-1 cells were released from a double thymidine block into 10 μM VS compounds, 10 μM monastrol or an equivalent volume of DMSO for 14 h. As a positive control, mitotic arrest was induced by releasing thymidine-arrested cells into 500 nM of the tubulin poison nocodazole for 14 h. Treated cells were fixed and stained with Hoechst 33342 dye to visualise the chromatin. The intensity of the chromatin stain was used to determine the cell-cycle profile by laser-scanning microscopy.

Table 2. IC_{50} and EC_{50} values of the more potent VS compounds.

Compounds	IC_{50} (EC_{50}[a])	Compounds	IC_{50} (EC_{50}[a])	Compounds	IC_{50} (EC_{50}[a])
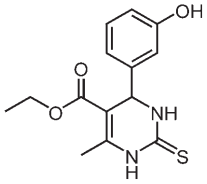 monastrol	20.73 ± 0.75 (58.74±2.60)	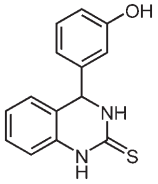 **VS-12**	7.60 ± 1.38 (22.51±0.79)	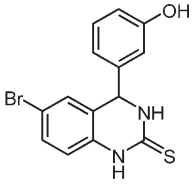 **VS-17**	5.75 ± 0.66 (24.49±1.56)
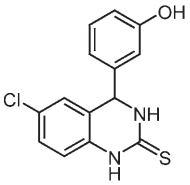 **VS-42**	5.77 ± 0.66 (20.60±0.55)	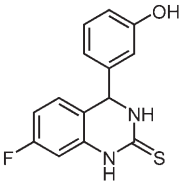 **VS-54**	1.81 ± 0.15 (8.51±0.22)	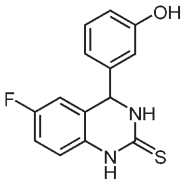 **VS-77**	8.04 ± 1.71 (28.39±2.74)
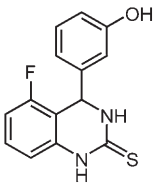 **VS-83**	1.17 ± 0.31 (7.27±0.83)	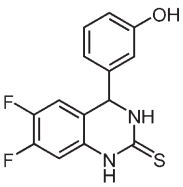 **VS-87**	2.74 ± 0.17 (8.95±0.31)	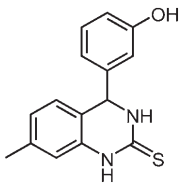 **VS-91**	7.59 ± 2.26 (25.09±0.94)
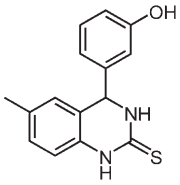 **VS-94**	2.73 ± 0.51 (12.92±0.64)				

[a] Concentration at which 50% of mitotic cells show monoasters.

2-Amino-4-fluoro-*N*-methoxy-*N*-methylbenzamide (6c): Yield: 97% for two steps. Oil. ^{1}H NMR (300 MHz, $CDCl_3$): $\delta = 3.32$ (s, 3H), 3.55 (s, 3H), 4.71 (br, 2H), 6.32–6.38 (m, 2H), 7.37–7.41 (m, 1H); ESI-HRMS *m/z* calcd for $C_9H_{11}F\ N_2O_2Na$: 221.06968 $[M+Na]^+$; found: 221.06982.

2-Amino-5-fluoro-*N*-methoxy-*N*-methylbenzamide (6d): Yield: 90% for two steps. Oil. ^{1}H NMR (200 MHz, $CDCl_3$): $\delta = 3.31$ (s, 3H), 3.55 (s, 3H), 4.31 (br, 2H), 6.62 (dd, $J = 8.8$, 4.8 Hz, 1H), 6.90 (m, 1H), 7.09 (dd, $J = 9.2$, 2.9 Hz, 1H); ESI-HRMS *m/z* calcd for $C_9H_{11}FN_2O_2$: 199.08773 $[M+H]^+$; found: 199.08777.

2-Amino-6-fluoro-*N*-methoxy-*N*-methylbenzamide (6e): Yield: 93% for two steps. Oil. ^{1}H NMR (200 MHz, $CDCl_3$): $\delta = 3.28$ (s, 3H), 3.58 (s, 3H), 4.21 (br, 2H), 6.34–6.45 (m, 2H), 7.05 (dd, $J = 14.8$, 7.7 Hz, 1H); ESI-HRMS *m/z* calcd for $C_9H_{12}FN_2O_2$: 199.08773 $[M+H]^+$; found: 199.08764.

2-Amino-4,5-difluoro-*N*-methoxy-*N*-methylbenzamide (6f): Yield: 70% for two steps. Oil. ^{1}H NMR (200 MHz, $CDCl_3$): $\delta = 3.32$ (s, 3H), 3.54 (s, 3H), 4.66 (br, 2H), 6.47 (d, $J = 12.1$, 6.9 Hz, 1H), 7.30 (dd, $J = 11.1$, 9.1 Hz, 1H); ESI-HRMS *m/z* calcd for $C_9H_{11}F_2N_2O_2$: 217.07831 $[M+H]^+$; found: 217.07834.

2-Amino-*N*-methoxy- *N*,3-dimethylbenzamide (6g): Yield: 73% for two steps. Oil. ^{1}H NMR (300 MHz, $CDCl_3$): $\delta = 2.1$ (s, 3H), 3.32 (s, 3H), 3.57 (s, 3H), 4.60 (br, 2H), 6.60 (t, $J = 7.1$ Hz, 1H), 7.06 (d, $J = 7.1$ Hz, 1H), 7.2 (d, $J = 7.1$ Hz, 1H); ^{13}C NMR, 75 MHz ($CDCl_3$): $\delta =$ 17.8, 34.9, 61.3, 116.6, 117.1, 123.4, 127.2, 132.6, 145.1, 170.8; ESI-HRMS *m/z* calcd for $C_{10}H_{14}N_2O_2Na$: 217.09475 $[M+Na]^+$; found: 217.09468.

2-Amino-*N*-methoxy-*N*,4-dimethylbenzamide (6h): Yield: 80% for two steps. Oil. ^{1}H NMR (200 MHz, $CDCl_3$): $\delta = 2.23$ (s, 3H), 3.30 (s, 3H), 3.56 (3H,s), 4.59 (br, 2H), 6.45–6.49 (m, 2H), 7.25 (d, $J = 7.7$ Hz, 1H); ^{13}C NMR (50 MHz, $CDCl_3$): $\delta = 21.5$, 34.6, 61.1, 114.3, 117.2, 117.9, 129.4, 141.9, 147.2, 170.4; ESI-HRMS *m/z* calcd for $C_{10}H_{14}N_2O_2$: 195.11280 $[M+H]^+$; found: 195.11281.

2-Amino-*N*-methoxy-*N*,5-dimethylbenzamide (6i): Yield: 90% for two steps. Oil. ^{1}H NMR (200 MHz, $CDCl_3$): $\delta = 2.23$ (s, 3H), 3.33 (s, 3H), 3.60 (s, 3H), 4.32 (br, 2H), 6.62 (d, $J = 8.1$ Hz, 1H), 6.99 (dd, $J = 8.1$, 1.1 Hz, 1H), 7.13 (d, $J = 1.1$ Hz, 1H); ^{13}C NMR (50 MHz, $CDCl_3$): $\delta = 20.4$, 34.5, 61.2, 116.9, 118.0, 126.3, 129.2, 132.2, 144.0, 170.2; ESI-HRMS *m/z* calcd for $C_{10}H_{14}N_2O_2$: 195.11280 $[M+H]^+$; found: 195.11292.

2-Amino-5-bromo-*N*-methoxy-*N*-methylbenzamide (6j): Yield: 97% for two steps as a solid. M.p. = 72–74 °C; ^{1}H NMR (200 MHz, $CDCl_3$): $\delta = 3.33$ (s, 3H), 3.58 (s, 3H), 4.68 (br, 2H), 6.61 (d, $J = 8.8$ Hz, 1H), 7.25 (dd, $J = 2.6$, 8.8 Hz, 1H), 7.49 (d, $J = 2.6$ Hz, 1H); ^{13}C NMR (50 MHz, $CDCl_3$): $\delta = 34.0$, 61.4, 108.3, 118.3, 118.7, 131.7, 134.2, 146.0, 168.6 ESI-HRMS *m/z* calcd for $C_9H_{11}BrN_2NaO_2$: 280.98961 $[M+Na]^+$; found: 280.98980.

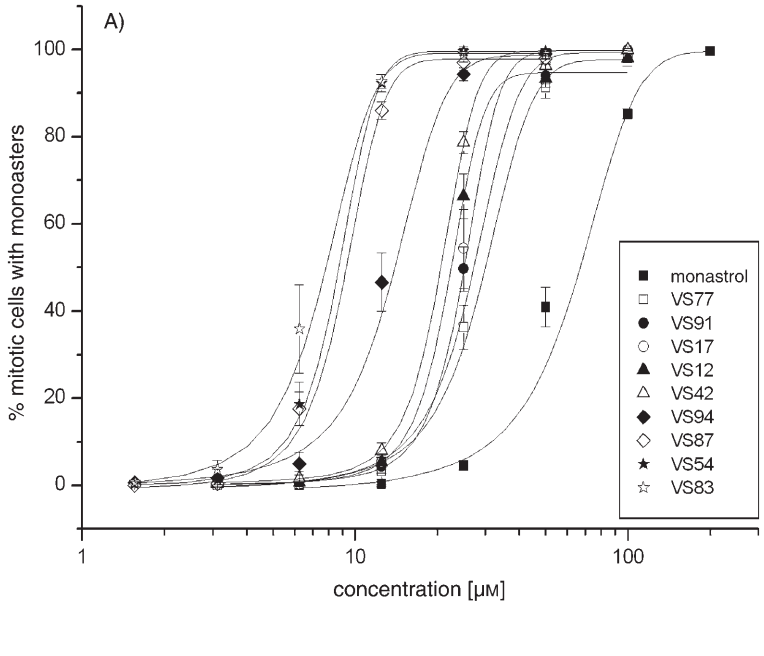

Figure 3. A) VS compounds induce the formation of monoasters in BSC-1 cells. BSC-1 cells were released from a double thymidine block into the indicated concentrations of VS compounds or monastrol for 10 h. Treated cells were fixed and immunostained for the microtubule cytoskeleton and chromatin. For each concentration of the tested compounds, the spindle structures of about 400 mitotic cells were determined. B) Graph A was used to determine the concentration of each compound at which 50% of the mitotic cells display a monoaster (EC_{50} value).

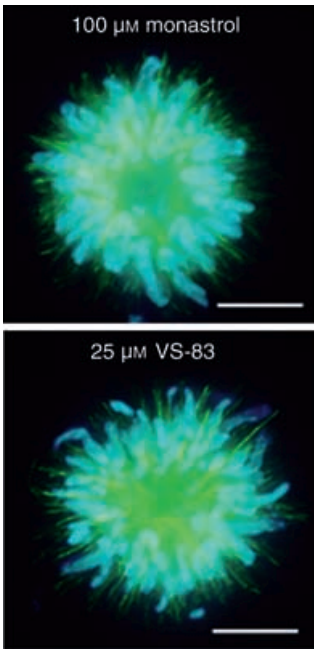

Figure 4. Immunofluorescence images of mitotic BSC-1 cell treated with A) VS-83 or B) monastrol. BSC-1 cells were released from a double thymidine block into 25 μM VS-83 or 100 μM monastrol for 10 h. Treated cells were fixed and immunostained for the microtubule cytoskeleton and chromatin. Images were taken on a Nikon TE-200 microscope equipped with a 100× lens and deconvolved by using Applied Precision Software.

2-Amino-*N*-methoxy-*N*-methylbenzamide (6k): Physical and spectroscopic data are in agreement with previously published data.[17]

(2-Amino-5-chlorophenyl) (3′-*tert*-butyldimethylsilyloxyphenyl)-methanone (7a): Yield: 75%. Oil. ^{1}H NMR (300 MHz, $CDCl_3$): δ = 0.23 (s, 6H), 0.99 (s, 9H), 6.04 (br, 2H), 6.67 (d, J = 8.8 Hz, 1H), 7.01–7.04 (m, 1H), 7.07–7.09 (m, 1H), 7.19–7.26 (m, 2H), 7.33 (t, J = 7.7 Hz, 1H), 7.44 (d, J = 2.5 Hz, 1H); ^{13}C NMR, 75 MHz ($CDCl_3$): δ = −4.1, 18.5, 25.9, 118.7, 119.0, 120.2, 120.8, 122.4, 123.7, 129.7, 133.5, 134.5, 140.9, 149.6, 155.8, 197.9; ESI-HRMS *m/z* calcd for $C_{19}H_{25}ClNO_2Si$: 362.13376 $[M+H]^+$; found: 362.13381.

(2-Amino-3-methoxyphenyl) (3′-*tert*-butyldimethyloxyphenyl)methanone (7b): Yield: 65%. Oil. ^{1}H NMR (200 MHz, $CDCl_3$): δ = 0.23 (s, 6H), 1.00 (s, 9H), 3.90 (s, 3H), 6.37 (br, 2H), 6.50–6.62 (m, 2H), 6.82–6.90 (t, J = 8.1 Hz, 1H), 6.98–7.02 (m, 1H), 7.09–7.12 (m, 1H), 7.20–7.41 (m, 2H); ^{13}C NMR (50 MHz, $CDCl_3$): δ = −4.3, 18.3, 25.8, 55.9, 113.8, 114.0, 117.5, 120.6, 122.2, 122.7, 122.8, 126.1, 129.1, 141.8, 147.4, 155.4, 198.7; ESI-HRMS *m/z* calcd for $C_{20}H_{27}NO_3Si$: 358.18330 $[M+H]^+$; found: 358.18324.

(2-Amino-4-fluorophenyl) (3′-*tert*-butyldimethylsilyloxyphenyl)methanone (7c): Yield: 88%. Oil. ^{1}H NMR (300 MHz, $CDCl_3$): δ = 0.21 (s, 6H), 0.98 (s, 9H), 6.26–6.32 (m, 3H), 6.36 (d, J = 2.5, 10.9 Hz, 1H), 6.98–7.05 (m, 2H), 7.17 (d, J = 7.4 Hz, 1H), 7.26–7.33 (m, 1H), 7.47 (dd, J = 6.6, 8.8 Hz, 1H); ESI-HRMS *m/z* calcd for $C_{19}H_{25}F\ NO_2Si$: 346.16331 $[M+H]^+$; found: 346.16336.

(2-Amino-5-fluorophenyl) (3′-*tert*-butyldimethylsilyloxyphenyl)-methanone (7d): Yield: 93%. Oil. ^{1}H NMR (200 MHz, $CDCl_3$): δ = 0.21 (s, 6H), 0.98 (s, 9H), 5.64 (br, 2H), 6.69 (dd, J = 8.9, 4.4 Hz, 1H), 7.02–7.36 (m, 6H); ESI-HRMS *m/z* calcd for $C_{19}H_{25}FNO_2Si$: 346.16331 $[M+H]^+$; found: 346.16309.

(2-Amino-6-fluorophenyl) (3′-*tert*-butyldimethylsilyloxyphenyl)-methanone (7e): Yield 85%. Oil. ^{1}H NMR (200 MHz, $CDCl_3$): δ = 0.19 (s, 6H), 0.97 (s, 9H), 4.72 (br, 2H), 6.37 (dd as t, J = 8.4 Hz, 1H), 6.52 (d, J = 8.4 Hz, 1H), 7.02 (d, J = 7.3 Hz, 1H), 7.14–7.32 (m, 4H); ESI-HRMS *m/z* calcd for $C_{19}H_{25}FNO_2Si$: 346.16331 $[M+H]^+$; found: 346.16332.

(2-Amino-4,5-difluorophenyl) (3′-*tert*-butyldimethylsilyloxyphenyl)methanone (7f): Yield: 93%. Oil. ^{1}H NMR (200 MHz, $CDCl_3$): $\delta =$ 0.21 (s, 6H), 0.99 (s, 9H), 6.06 (br, 2H), 6.50 (dd, $J = 11.8$, 6.6 Hz, 1H), 7.00–7.18 (m, 3H), 7.27–7.35 (m, 2H); ESI-HRMS *m/z* calcd for $C_{19}H_{24}F_2NO_2Si$: 364.15389 $[M+H]^+$; found: 364.15378.

(2-Amino-3-methylphenyl) (3′-*tert*-butyl-dimethylsilyloxyphenyl)methanone (7g): Yield: 57%. Oil. ^{1}H NMR (300 MHz, $CDCl_3$): $\delta =$ 0.22 (s, 6H), 1.00 (s, 9H), 2.22 (s, 3H), 6.21 (br, 2H), 6.55 (dd as t, $J = 7.7$ Hz, 1H), 6.99–7.02 (m, 1H), 7.11 (m, 1H), 7.21–7.33 (m, 3H), 7.38 (d, $J = 7.4$ Hz, 1H); ^{13}C NMR, 75 MHz ($CDCl_3$): $\delta = -4.1$, 17.6, 18.5, 26.0, 115.1, 117.8, 120.9, 122.5, 123.0, 123.5, 129.4, 133.1, 135.4, 142.1, 149.7, 155.6, 199.5; ESI-HRMS *m/z* calcd for $C_{20}H_{28}NO_2Si$: 342.18838 $[M+H]^+$; found: 342.18854.

(2-Amino-4-methylphenyl) (3′-*tert*-butyl-dimethylsilyloxyphenyl)methanone (7h): Yield: 70%. Oil. ^{1}H NMR (300 MHz, $CDCl_3$): $\delta =$ 0.21 (s, 6H), 0.98 (s, 9H), 2.29 (s, 3H), 6.15 (br, 2H), 6.43 (d, $J =$ 8.0 Hz, 1H), 6.56 (br s, 1H), 6.97–7.20 (m, 3H), 7.27–7.37 (m, 2H); ^{13}C NMR (50 MHz, $CDCl_3$): $\delta = -4.3$, 18.3, 21.9, 25.8, 112.7, 116.0, 117.2, 120.6, 122.1, 122.7, 129.2, 134.9, 141.9, 145.5, 151.2, 155.4, 198.4; ESI-HRMS *m/z* calcd for $C_{20}H_{28}NO_2Si$: 342.18838 $[M+H]^+$; found: 342.18836.

(2-Amino-5-methylphenyl) (3′-*tert*-butyl-dimethylsilyloxyphenyl)methanone (7i): Yield: 92%. Oil. ^{1}H NMR (200 MHz, $CDCl_3$): $\delta = 0.21$ (s, 6H), 0.98 (s, 9H), 2.17 (s, 3H), 5.60 (br, 2H), 6.67 (d, $J = 8.4$ Hz, 1H), 6.98–7.14 (m, 3H), 7.20–7.35 (m, 3H); ^{13}C NMR (50 MHz, $CDCl_3$): $\delta = -4.2$, 18.4, 20.5, 25.9, 117.4, 118.4, 120.8, 122.4, 123.1, 124.9, 129.5, 134.3, 135.7, 141.7, 148.9. 155.5, 198.9; ESI-HRMS *m/z* calcd for $C_{20}H_{28}NO_2Si$: 364.18838 $[M+H]^+$; found: 342.18835.

(2-Amino-5-bromophenyl) (3′-*tert*-butyldimethylsilyloxyphenyl)methanone (7j): Yield: 82%. Oil. ^{1}H NMR (300 MHz, $CDCl_3$): $\delta = 0.24$ (s, 6H), 0.99 (s, 9H), 6.10 (br, 2H), 6.63 (d, $J = 8.5$ Hz, 1H), 7.01–7.07 (m, 2H), 7.19–7.36 (m, 3H), 7.57 (br s, 1H); ^{13}C NMR (75 MHz, $CDCl_3$): $\delta = -4.3$, 18.2, 25.7, 106.5, 118.8, 119.3, 120.5, 122.1, 123.4, 129.4, 136.2, 136.8, 140.5, 149.7, 155.5, 197.5; ESI-HRMS *m/z* calcd for $C_{19}H_{25}BrNO_2Si$: 406.08324 $[M+H]^+$; found: 406.08343.

(2-Aminophenyl) (3′-*tert*-butyldimethylsilyloxyphenyl)methanone (7k): Yield: 66%: Oil. ^{1}H NMR (200 MHz, $CDCl_3$): $\delta = 0.22$ (s, 6H), 0.99 (s, 9H), 6.11 (br, 2H), 6.57–6.65 (m, 1H), 6.74 (d, $J = 8.4$, 1H), 7.01 (m, 1H), 7.10 (m, 1H), 7.19–7.36 (m, 3H), 7.47 (dd, $J = 1.5$, 8.1 Hz, 1H); ^{13}C NMR (50 MHz, $CDCl_3$): $\delta = -4.2$, 18.4, 25.8, 115.6, 117.1, 118.3, 120.7, 122.3, 123.0, 129.3, 134.4, 134.8, 141.6, 151.1, 155.5, 198.9; ESI-HRMS *m/z* calcd for $C_{19}H_{26}NO_2Si$: 328.17273 $[M+H]^+$; found: 328.17280.

3,4-Dihydro-4-phenylquinazoline-2(1*H*)-thione (VS-1): Physical and spectroscopic data are in agreement with previously published data.[18]

3,4-Dihydro-4-(3′-hydroxyphenyl)quinazoline-2(1*H*)-thione (VS-12): Yield: 74%. M.p. = 217–219 °C; ^{1}H NMR (200 MHz, DMSO): $\delta =$ 5.52 (, 1Hd, $J = 3.0$ Hz), 6.64–6.75 (m, 3H), 6.97–7.00 (m, 2H), 7.03–7.20 (m, 3H), 9.19 (br, 1H), 9.50 (s, 1H), 10.65 (br, 1H); ^{13}C NMR (50 MHz, DMSO): $\delta = 56.6$, 113.1, 114.2, 114.5, 116.8, 121.2, 123.0, 126.9, 128.1, 129.5, 134.1, 145.7, 157.5, 174.4; ESI-HRMS *m/z* calcd for $C_{14}H_{13}N_2OS$ $[M+H]^+$ 257.07431; found: 257.07419.

6-Bromo-3,4-dihydro-4-(3′-hydroxyphenyl)quinazoline-2(1*H*)-thione (VS-17): Yield: 90%. M.p. = 115–117 °C; ^{1}H NMR (300 MHz, DMSO): $\delta = 5.55$ (d, $J = 3.0$ Hz, 1H), 6.67–6.69 (m, 2H), 6.74 (d, $J =$ 7.7 Hz, 1H), 6.98 (d, $J = 8.5$ Hz, 1H), 7.13–7.16 (m, 1H), 7.37–7.41 (m, 2H), 9.31 (br, 1H), 9.55 (s, 1H), 10.78 (br, 1H); ^{13}C NMR, 75 MHz (DMSO): $\delta = 56.7$, 113.7, 115.0, 115.5, 117.0, 117.5, 124.4, 130.1, 130.5, 131.7, 134.2, 146.0, 158.4, 175.3; ESI-HRMS *m/z* calcd for $C_{14}H_{12}BrN_2OS$: 334.98482 $[M+H]^+$; found: 334.98416.

3,4-Dihydro-4-(3′-hydroxyphenyl)-8-methylquinazoline-2(1*H*)-thione (VS-38): Yield: 83%. M.p. = 25–256 °C; ^{1}H NMR (300 MHz, DMSO): $\delta = 2.31$ (s, 3H), 5.49 (d, $J = 3.3$ Hz, 1H), 6.66–6.68 (m, 2H), 6.74 (d, $J = 7.7$ Hz, 1H), 6.93 (dd as t, $J = 7.4$ Hz, 1H), 7.03–7.16 (m, 3H), 9.33 (br, 1H), 9.49 (s, 1H), 9.52 (br, 1H); ^{13}C NMR, 75 MHz (DMSO): $\delta = 17.8$, 57.4, 113.9, 115.2, 117.5, 122.6, 123.4, 123.8, 125.5, 130.2, 130.6, 133.1, 146.1, 158.2, 176.0. EI-HRMS *m/z* calcd for $C_{15}H_{14}N_2OS$: 270.08268 $[M]^+$; found: 270.08101.

6-Chloro-3,4-dihydro-4-(3′-hydroxyphenyl)quinazoline-2(1*H*)-thione (VS-42): Yield: 70%. M.p. = 108–110 °C; ^{1}H NMR (300 MHz, DMSO): $\delta = 5.55$ (d, $J = 3.3$ Hz, 1H), 6.68–6.69 (m, 2H), 6.75 (d, $J =$ 7.5 Hz, 1H), 7.04 (d, $J = 9.0$ Hz, 1H), 7.14–7.19 (m, 1H), 7.26–7.29 (m, 2H), 9.30 (br, 1H), 9.56 (s, 1H), 10.79 (br, 1H); ^{13}C NMR (50 MHz, DMSO): $\delta = 56.1$, 113.0, 114.7, 115.9, 116.7, 123.3, 126.4, 126.5, 128.1, 129.7, 133.1, 145.2, 157.6, 174.5; ESI-HRMS *m/z* calcd for $C_{14}H_{12}ClN_2OS$: 291.03534 $[M+H]^+$; found: 291.03518.

6-Chloro-3,4-dihydro-4-phenylquinazoline-2(1*H*)-thione (VS-43): Yield: 97%. M.p. = 225–227 °C; ^{1}H NMR (300 MHz, DMSO), $\delta = 5.66$ (d, $J = 3.3$, 1H), 7.05 (d, $J = 8.4$ Hz, 1H), 7.26–7.41 (m, 6H), 9.36 (s, 1H), 10.8 (s, 1H); ^{13}C NMR (75 MHz, DMSO): $\delta = 56.9$, 116.7, 124.0, 126.9, 127.3, 128.5, 129.0, 129.5, 133.9, 144.5, 175.4; ESI-HRMS *m/z* calcd for $C_{14}H_{12}ClN_2S$ $[M+H]^+$ 275.04042; found: 275.04086.

6-Chloro-4-(2′-fluorophenyl)-3,4-dihydroquinazoline-2(1*H*)-thione (VS-46): Yield: 94%. M.p. = 279–281 °C; ^{1}H NMR (300 MHz, DMSO): $\delta = 5.92$ (d, $J = 2.8$ Hz, 1H), 7.03–7.07 (m, 2H), 7.22–7.43 (m, 5H), 9.23 (br, 1H), 10.88 (br, 1H); ESI-HRMS *m/z* calcd for $C_{14}H_{11}ClFN_2OS$: 293.03100 $[M+H]^+$; found: 293.03101.

3,4-Dihydro-4-(3′-hydroxyphenyl)-8-methoxyquinazoline-2(1*H*)-thione (VS-48): Yield: 84%. M.p. = 254–256 °C; ^{1}H NMR (300 MHz, DMSO): $\delta = 3.86$ (s, 3H), 5.52 (d, $J = 3.0$ Hz, 1H), 6.67–6.78 (m, 4H), 6.93–7.02 (m, 2H), 7.11–7.16 (m, 1H), 8.83 (br, 1H), 9.38 (br, 1H), 9.51 (s, 1H); ^{13}C NMR (50 MHz, DMSO): $\delta = 56.6$, 55.9, 110.1, 113.1, 114.5, 116.8, 118.6, 121.8, 123.0, 123.5, 129.5, 144.7, 145.1, 157.5, 174.2; ESI-HRMS *m/z* calcd for $C_{15}H_{14}N_2O_2SNa$: 309.06682 $[M+Na]^+$; found: 309.06711.

7-Fluoro-3,4-dihydro-4-(3′-hydroxyphenyl)quinazoline-2(1*H*)-thione (VS-54): Yield: 89%. M.p. = 85–87 °C; ^{1}H NMR (300 MHz, DMSO): $\delta = 5.53$ (d, $J = 3.0$ Hz, 1H), 6.66–6.84 (m, 5H), 7.12–7.20 (m, 2H), 9.34 (br, 1H), 9.51 (s, 1H), 10.74 (br, 1H); ESI-HRMS *m/z* calcd for $C_{14}H_{11}F\ N_2OSK$: 313.02077 $[M+K]^+$; found: 313.02087.

6-Fluoro-3,4-dihydro-4-(3′-hydroxyphenyl)quinazoline-2(1*H*)-thione (VS-77): Yield 84%. M.p. = 166–168 °C; ^{1}H NMR (200 MHz, DMSO): $\delta = 5.51$ (d, $J = 3.0$ Hz, 1H), 6.64–6.74 (m, 3H), 7.03–7.16 (m, 4H), 9.2 (br, 1H), 9.51 (s, 1H), 10.70 (br, 1H); ESI-HRMS *m/z* calcd for $C_{14}H_{12}FN_2OS$: 275.06489 $[M+H]^+$; found: 275.06478.

5-Fluoro-3,4-dihydro-4-(3′-hydroxyphenyl)quinazoline-2(1*H*)-thione (VS-83): Yield: 89%. M.p. = 215–217 °C; ^{1}H NMR (200 MHz, DMSO): $\delta = 5.54$ (d, $J = 2.2$ Hz, 1H), 6.60–6.66 (m, 3H), 6.74–6.88 (m, 2H), 7.08–7.30 (m, 2H), 9.34 (br, 1H), 9.51 (s, 1H), 10.85 (br, 1H); ESI-HRMS *m/z* calcd for $C_{14}H_1FN_2OSNa$: 297.04683 $[M+Na]^+$; found: 297.04664.

6,7-Difluoro-3,4-dihydro-4-(3′-hydroxyphenyl)quinazoline-2(1*H*)-thione (VS-87): Yield: 90%. M.p. = 237–240 °C; ^{1}H NMR (300 MHz, DMSO): $\delta = 5.49$ (d, $J = 2.4$ Hz, 1H), 6.68–6.76 (m, 3H), 6.98 (dd, $J =$ 11.3, 7.1 Hz, 1H), 7.14 (dd as t, $J = 7.7$ Hz, 1H), 7.30 (dd, $J = 8.5$ Hz, 1H), 9.33 (br, 1H), 9.52 (s, 1H), 10.73 (br, 1H); ESI-HRMS *m/z* calcd for $C_{14}H_{11}F_2N_2OS$: 293.05547 $[M+H]^+$; found: 293.05535.

3,4-Dihydro-4-(3-hydroxyphenyl)-7-methylquinazoline-2(1*H*)-thione (VS-91): Yield: 83%. M.p. = 231–233 °C; ^{1}H NMR (200 MHz, DMSO): $\delta = 2.20$ (s, 3H), 5.44 (d, $J = 2.9$ Hz, 1H), 6.61–6.79 (m, 5H), 6.96–7.15 (m, 2H), 9.09 (br, 1H), 9.44 (s, 1H), 10.55 (br, 1H); ^{13}C NMR (50 MHz, DMSO): $\delta = 20.8$, 56.5, 113.1, 114.4, 116.8, 116.9, 118.4, 123.8, 126.8, 129.5, 134.0, 137.5, 145.9, 157.5, 174.4; ESI-HRMS *m/z* calcd for $C_{15}H_{15}N_2OS$: 271.08996 $[M+H]^+$; found: 271.09006.

3,4-Dihydro-4-(3-hydroxyphenyl)-6-methylquinazoline-2(1*H*)-thione (VS-94): Yield: 80%. M.p. = 249–252 °C; ^{1}H NMR (200 MHz, DMSO): $\delta = 2.14$ (s, 3H), 5.40 (d, $J = 3.0$ Hz, 1H), 6.62–6.85 (m, 3H), 6.88–7.14 (m, 4H), 9.05 (br, 1H), 9.45 (s, 1H), 10.54 (br, 1H); ^{13}C NMR (50 MHz, DMSO): $\delta = 21.1$, 57.4, 113.8, 114.9, 115.2, 117.6, 121.8, 127.8, 129.4, 130.3, 132.5, 132.7, 146.6, 158.2, 174.7; ESI-HRMS *m/z* calcd for $C_{15}H_{14}N_2OSNa$: 293.07190 $[M+Na]^+$; found: 293.07197.

Cell culture and immunofluorescence: BSC-1 (African green monkey) cells were cultured in DMEM media (Invitrogen/Gibco), supplemented with 10% foetal calf serum and penicillin/streptomycin (1 U, Gibco, Germany) at 37 °C and under 5% CO_2. To determine the number of mitotic cells with monoasters and for cell-cycle profile analyses, cells were synchronised using a double thymidine block. In brief, cells were plated on cover slips (Marienfeld) and cultured in the presence of 2 mM thymidine (Sigma) for 18 h. Six hours after the first release from the thymidine block, cells were treated again with 2 mM thymidine for 18 h. After the second release cover slips were transferred to a 24 well plate, containing 300 μL culture media, supplemented with chemical compounds or equivalent volume of DMSO (1% final concentration) as a solvent control. Plates were returned to the incubator and at the indicated time points cover slips were processed for further analyses.

To prepare cells for immunofluorescence, the medium was replaced by permeabilisation buffer (100 mM K-Pipes, 1 mM ethyleneglycol bis(2-aminoethylether)-*N,N,N′,N′*-tetraacetic acid (EGTA), 1 mM $MgCl_2$, 0.2% Triton-X 100). After 10 min of incubation, cells were washed with TBS-TX buffer (10 mM Tris, pH 7.5, 100 mM NaCl, 0.1% Triton-X 100) followed by 1 h of incubation in antibody dilution buffer (AbDil.: TBS-TX, 2% BSA). Cells were then incubated for 1 h in antitubulin (1 g mL^{-1}, Sigma) in AbDil. After being washed with TBS-TX, cells were incubated for 10 min with Hoechst 33342 (1 μg mL^{-1}), washed again and embedded in mounting media (20 mM Tris·HCl pH 8.8; 0.5% phenylenediamine; 90% glycerol).

Microscopic analyses: Microscopic analyses of cells immunostained for microtubules and chromatin were performed on an upright microscope (Zeiss, Axioskope2) equipped with a 40× lens. Mitotic cells were identified on the basis of condensed chromosomes. To determine the number of mitotic cells with monoasters, the morphology of the spindle was analysed for 400 mitotic cells per compound concentration. To determine the cell-cycle profile, cells stained for chromatin were analysed on a light-scanning microscope (CompuCyte) equipped with a 20× lens as described previously.[20] High-quality images of compound-treated cells were acquired on an inverse Nikon TE-200 microscope equipped with a 100× lens and images were deconvoluted by using the Applied Precision deconvolution software.[25]

Enzymatic assays: The kinesin motor domain of Eg5 was cloned by a PCR from a testis cDNA library (Invitrogene) by using the following primers: 5′: ATGGCGTCGCAGCCAAATT, 3′: AGTTTCTGATTCACTTCAGGCT. PCR constructs were cloned into pQE80 expression vector with an N-terminal His-tag. Recombinant protein was expressed in *E. coli* strain JM109^{RIL} purified over a NiTA (Qiagen) column, dialysed against storage buffer (25 mM Tris, pH 7,4 150 mM NaCl, 10 mM mercaptoethanol and 10% glycerol) and stored at −80 °C.

Tubulin was purified from pig brain as described before[24] and stored at −80 °C in BRB80 (80 mM K-Pipes, pH 6,8, 1 mM EGTA, 1 mM $MgCl_2$). Microtubules were polymerised as described previously.[23]

The ATPase activity of the Eg5 motor domain was measured by using the malachite green assay as described.[19] The reactions were performed in reaction buffer (80 mM Pipes, pH 6,8; 1 mM EGTA, 1 mM $MgCl_2$, 0,1 mg mL^{-1} BSA, 1 μM taxol) supplemented with the Eg5 (48 nM) fusion protein and microtubules (200 nM). 10 min after compound addition, reactions were started by the addition of ATP (50 μM) and incubated at RT for 7 min. The reactions were stopped by adding perchloric acid (444 mM, Fluka), and the colour reaction was started by adding the developer solution (1 M HCl (Sigma), 33 μM malachite green (Sigma), 775 μM ammonium molybdate tetrahydrate (Sigma)). After 20 min, the absorbance at 610 nm was measured by using a plate reader (Victor2, Perkin–Elmer). The IC_{50} values were determined in three independent duplicate experiments.

Acknowledgements

This work was supported by Grant MRTN-CT-2004-512348 (Spindle Dynamics) from the European Commission. T.U.M. is a fellow of the Emmy–Noether Programm of the Deutschen Forschungsgemeinschaft; S.H. is a fellow of the Verband der Chemischen Industrie.

Keywords: ab initio calculations · Eg5 · inhibitors · kinesin · mitosis · spindle

[1] K. W. Wood, W. D. Cornwell, J. R. Jackson, *Curr. Opin. Pharmacol.* **2001**, *1*, 370–377.
[2] K. N. Bhalla, *Oncogene* **2003**, *22*, 9075–9086.
[3] J. P. Jaffrezou, C. Dumontet, W. B. Derry, G. Duran, G. Chen, E. Tsuchiya, L. Wilson, M. A. Jordan, B. J. Sikic, *Oncol. Res.* **1995**, *7*, 517–527.
[4] D. J. Sharp, G. C. Rogers, J. M. Scholey, *Nature* **2000**, *407*, 41–47.
[5] T. Wittmann, A. Hyman, A. Desai, *Nat. Cell Biol.* **2001**, *3*, E28–34.
[6] A. Desai, T. J. Mitchison, *Annu. Rev. Cell Dev. Biol.* **1997**, *13*, 83–117.
[7] T. U. Mayer, T. M. Kapoor, S. J. Haggarty, R. W. King, S. L. Shreiber, T. J. Mitchison, *Science* **1999**, *286*, 971–974.
[8] C. D. Cox, M. J. Breslin, B. J. Mariano, P. J. Coleman, C. A. Buser, E. S. Walsh, K. Hamilton, H. E. Huber, N. E. Kohl, M. Torrent, Y. Yan, L. C. Kuo, G. D. Hartman, *Bioorg. Med. Chem. Lett.* **2005**, *15*, 2041–2045.
[9] J. Nakazawa, J. Yajima, T. Usui, M. Ueki, A. Takatsuki, M. Imoto, Y. Y. Toyoshima, H. Osaka, *Chem. Biol.* **2003**, *10*, 131–137.
[10] S. Brier, D. Lemaire, S. DeBonis, E. Forest, F. Kozielski, *Biochemistry* **2004**, *43*, 13072–13082.
[11] S. Hotha, J. C. Yarrow, J. G. Yang, S. Garrett, K. Renduchintala, T. U. Mayer, T. M. Kapoor, *Angew. Chem.* **2003**, *115*, 2481–2484; *Angew. Chem. Int. Ed.* **2003**, *42*, 2379–2382.
[12] R. Sakowicz, J. T. Finer, C. Beraud, A. Crompton, E. Lewis, A. Fritsch, Y. Lee, J. Mak, R. Moody, R. Turincio, J. C. Chabala, P. Gonzales, S. Roth, S. Weitman, K. W. Wood, *Cancer Res.* **2004**, *64*, 3276–3280.
[13] M. Gartner, N. Sunder-Plassmann, J. Seiler, M. Utz, I. Vernos, T. Surrey, A. Giannis, *ChemBioChem*, **2005**, *6*, 1173–1177.
[14] P. R. Gerber, K. Muller, *J. Comput.-Aided Mol. Des.* **1995**, *9*, 251–268.
[15] P. R. Gerber, *J. Comput.-Aided Mol. Des.* **1998**, *12*, 37–51.
[16] M. H. Normal, G. C. Rigdon, W. R. Hall, F. Navas, *J. Med. Chem.* **1996**, *39*, 1172–1188.
[17] S. V. Frye, M. C. Johnson, N. L. Valvano, *J. Org. Chem.* **1991**, *56*, 3750–3752.

[18] D. Xu, P. G. Kucerovy, K. Prasad, O. Repic, *Tetrahedron: Asymmetry* **1996**, *7*, 747 – 754.
[19] R. D. Henkel, J. L. VandeBerg, R. A. Walsh, *Anal. Biochem.* **1988**, *169*, 312 – 318.
[20] L. A. Kamentsky, *Methods Cell Biol.* **2001**, *63*, 51 – 87.
[21] A. I. Marcus, U. Peters, S. L. Thomas, S. Garrett, A. Zelnak, T. Kapoor, P. Giannakakou, *J. Biol. Chem.* **2005**, *280*, 11 569 – 11 577.
[22] S. A. Haque, T. P. Hasaka, A. D. Brooks, P. V. Lobanov, P. W. Baas, *Cell Motil. Cytoskeleton* **2004**, *58*, 10 – 16.
[23] H. Bringmann, G. Skiniotis, A. Spilker, S. Kandels-Lewis, I. Vernos, T. Surrey, *Science* **2004**, *303*, 1599.
[24] M. Castoldi, A. V. Popov, *Protein Expression Purif.* **2003**, *32*, 83 – 88.
[25] D. A. Agard, Y. Hiraoka, P. Shaw, J.W. Sedat, *Methods Cell Biol.* **1989**, *30*, 353 – 377.

Received: April 20, 2005
Published online on October 10, 2005

